Research Article

Ahmet Çoşgun*

Spatial mapping of indoor air quality in a light metro system using the geographic information system method

https://doi.org/10.1515/chem-2023-0208
received December 26, 2023; accepted February 9, 2024

Abstract: It is known that one of the greatest problems of developed countries in the twenty-first century is traffic. For this reason, engineers have searched for alternative solutions to the problem of traffic. One such solution is the construction and utilization of rail systems instead of main roads. From an engineering perspective, rail systems can be divided into three groups: metro, light metro, and tram systems. Light metro systems, which are a form of public transportation, are not directly inside the traffic. Their most important advantages include the fact that they do not release combustion products such as CO, and metro and light metro systems may be considered environmentally friendly based solely on their electricity consumption. In this study, measurements of parameters affecting indoor air quality were made inside light metro cars and in and around light metro stations belonging to the light metro system of the Metropolitan Municipality of Antalya, known as the tourism capital of Turkey. In February and March 2021, when the COVID-19 pandemic was first registered in Turkey, particulate matter (PM), temperature, and relative humidity measurements were made for testing indoor and outside air quality. Moreover, as outside air parameters, outside temperature, outside relative humidity, CO, normalized difference vegetation index, and ultraviolet aerosol index data were obtained from the General Directorate of Meteorology of Turkey. The measurement results were analyzed using the inverse distance weighting method in the geographic information system. Based on the results of the analyses, spatial maps were created for indoor and outside air quality parameters in the light metro system. Using these maps, the effects of passenger density and environmental factors both inside the metro cars and at the metro stations on indoor air quality were identified. In addition, the spread of the SARS-CoV-2 virus in the COVID-19 period was analyzed using spatial maps of the $PM_{0.3}$ and $PM_{0.5}$ parameters. It is believed that the results of this study will set an example for further indoor air quality studies worldwide, and this study is unique in that it employed a method that is used particularly in survey and geomatics engineering for analyzing indoor air quality in light metro systems.

Keywords: light metro, indoor air, temperature, humidity, PM, CO, NDVI, aerosols, GIS

1 Introduction

Rail systems are among the most preferred land transport vehicles for fast transportation. However, their initial investment costs are high compared to other forms of transportation. In general, they are the most prevalently employed mode of transportation in the capitals and metropolitan cities of countries. Rail systems can be divided into three groups: metro, light metro, and tram systems. Light metro systems are popular due to their speed in transportation and the comfort parameters they provide, including air conditioning parameters (temperature, relative humidity, air velocity, air distribution, and air purity). In contrast with metro systems, light metro systems mostly travel above ground on rails.

In large cities, individuals spend 4–8% of their day (1–2 h) commuting to and from work. As stated in several different studies, during this period, people are exposed to high concentrations of particulate matter (PM) [1].

The properties of a light metro system are presented in Table 1.

1.1 Previous studies on the topic

Several studies on indoor air quality have been carried out in the relevant literature for metro and light metro systems

* **Corresponding author: Ahmet Çoşgun,** Department of Mechanical Engineering, Faculty of Engineering, Akdeniz University, Campus, Antalya, Turkey, e-mail: acoskun@akdeniz.edu.tr
ORCID: Ahmet Çoşgun 0000-0002-0243-5476

Table 1: Properties of a light metro system [9]

Light metro system	Value/unit
Platform length	~100 m
Car width	2,650 mm
Rail type	S46 vignole rail
Energy supply	Rigid catenary or 3rd rail
Current	750 DC or 1500 DC
Commercial speed	42–45 km/h
Maximum speed	80 km/h
Maximum passenger capacity	35,000/direction
Total car length	20–33 m
Distance between stations	600–1,000 m

in Asia and Europe. In particular, some studies on PM values are presented in Table 2.

As seen in Table 2, PM values were investigated in metro systems for the first time in 1995. The aforementioned study was carried out in the London Underground, which was established in 1863, and a $PM_{2.5}$ concentration of 893 μg/m^3 was determined [2].

While PM values usually vary between 10 and 200 μg/m^3 in Asian countries, the highest PM measurements in Shanghai (respectively, PM_{10}, $PM_{2.5}$, and PM_1) were 366, 287, and 231 μg/m^3.

In the metro system of Athens in Greece, PM_1, $PM_{2.5}$, and PM_{10} measurements were made at fixed positions inside metro cars on the Blue Line in November 2014 and November 2015, and assessments were made according to the Directive 2008/50/EC of the European Parliament on air quality. PM_{10} measurements were made in two directions of travel on all routes during commuting hours. The PM_{10} concentration was found as 132.2 ± 34 μg/m^3 on the Red Line and 138.0 ± 35.6 μg/m^3 on the Blue Line. In Athens, where measurements were made on eight different lines, passenger density was observed to be high in stations located under the streets of the city center with high traffic. To calculate the accumulation and retention dose of aerosols in the respiratory tract (RT) and the gastrointestinal system and their uptake into the bloodstream, an exposure model was applied using the formula E*DoM^2. Consequently, while PM values were found lower inside metro cars with open windows, they were high especially when the windows were closed [3].

Previous studies have mostly made comparisons between indoor air quality parameters measured in metro, light metro, tram, and train cars and values in existing standards.

In Turkey, indoor air quality measurements for metro systems were made for the first time in 2007 by the Environmental Engineering Department of Istanbul University. In the study, PM_{10}, $PM_{2.5}$, Fe, and Cu measurements were analyzed [4].

In a review study in Turkey, studies conducted on indoor air quality on the platforms and in the cars of metro and other rail systems in Turkey and the rest of the world were examined. Indoor air quality measurements in metro and train cars in Turkey were compared to those in other countries by taking into account the properties of metro systems [5].

In a master's thesis titled "the Effects of Ventilation Systems on Indoor Air Quality in Metro Systems in Istanbul," $PM_{2.5}$ measurements were made in metro systems in Istanbul, and the concentrations to which the personnel and passengers were exposed were determined. By making comparisons between indoor and outside air quality measurements, the effects of metro ventilation systems on indoor air quality were examined. It was determined that indoor air quality in metro systems could be significantly improved by supporting metro ventilation systems with platform screen doors and improving outside air quality [4].

In a study conducted to investigate and model the effects of PM on indoor air quality in light metro systems in Antalya, Turkey, PM measurements were made in January, February, and March in 2012, and it was determined that there were differences between the values measured in the metro cars and those measured on the platforms [6].

In a presentation about traffic-related carbon black levels in Istanbul, Turkey, and their relationship to $PM_{2.5}$ concentrations, both in-vehicle and outside measurements were made in different transportation systems including buses, metrobuses, metros, automobiles, fast ferries, and ferries between June and September 2016. In the comparisons of the outside air quality measurements of three different metrobus stops (Zincirlikuyu, Avcılar, and Söğütlüçeşme), the highest mean black carbon concentrations in June, July, August, and September in Avcılar were 14.1 ± 10.4, 15.5 ± 17.6, 18.4 ± 12.2, and 15.3 ± 11.6 μg/m^3, respectively. In measurements made at two bus stops, the highest $PM_{2.5}$ concentrations in June, July, August, and September in Bakırköy were 4.5 ± 4.0, 8.2 ± 11.7, 9.8 ± 16.2, and 13.3 ± 33.1 μg/m^3, respectively [7].

There are also other studies on vehicles other than metro trains in Turkey. In one of such studies, a doctoral thesis on the experimental measurement of changes in thermal parameters and indoor air quality in automobile cabins, experiments were carried out under real climate conditions using different air conditioning and heating parameters. The temperatures of the solid surfaces of the cabin and human skin were measured using an infrared camera with the thermographic method, and real-time temperature distributions were determined during cooling and heating periods. As a result, mathematical models to analyze the fluid dynamics of thermal comfort parameters and the thermophysical interactions between individuals and their surroundings were developed [8].

Table 2: PM measurements made in rail systems in Asia and Europe [2]

Ctiy	Metro production year	Measurement year	Polluting	Average concentration
ASYA				
Hong Kong	1979	1995–96	CO, NOx	1,500, 205 ppb
		2014	PM10, PM2.5	120; 10.2 μg/m^3
Beijing	1969	2004	TVOC	0.3 ppm
			TSP, PM10, PM2.5, PM1	166; 108; 36.9; 14.7
			Benzen, Toluen, Xylen	μg/m^3
		2005	Karbonlu Bileşenler	13.7; 12.4; 4.1 μg/m^3
		2007	Bakteri ve Mantar	98.5 μg/m^3
		2011	PAHs	12,639; 1,806 CFU/m^3
				50.3 ng/m^3
Shanghai	1993	2008	PM10, PM2.5, PM1	366; 287; 231 μg/m^3
		2008	Karbonlu Bileşenler	24 μg/m^3
		2015	Siyah Karbon	9.43 μg/m^3
Guangzhou	1997	2002	PM10, PM2.5	55; 44 μg/m^3
		2000	Volatile organic compounds (VOC)	60.5 μg/m^3
Tianjin	1984	2015	PM2.5	151.4 μg/m^3
Taipei	1996	2011	PM10, PM2.5	58; 32 μg/m^3
Seoul	1971	2007–2008	PM10, PM2.5	150; 118 μg/m^3
		2005	Fe	70%
		2015	Bakteri, Mantar	210; 75 CFU/m^3
		2006	VOC	146.7 μg/m^3
Tokyo	1927	2004	Mantar	342 CFU/m^3
		1997	TSP	90 μg/m^3
Tehran	1986	2011	Mantar	1,210 CFU/m^3
		2015–2016 [2]	PM10, PM2.5	33–102; 40–98 μg/m^3
Delhi	2002	2012	PM2.5	78 μg/m^3
St.Petersburg	1935	2007	Bakteri ve Mantar	2,236; 205 CFU/m^3
AMERİKA				
Boston	1897	1990	VOC	12.5 μg/m^3
Washington	1976	1999	PM	10^6 adet/m^3
New York	1907	1999	Fe, Cr, Mn	500; 84; 240 ng/m^3
		2007	PM2.5	30.6 μg/m^3
Los Angeles	1990	2012	PM	27,500 adet/m^3
		2010	PM10, PM2.5	78; 56.7 μg/m^3
		2011	PAHs	3,693 μg/m^3
Mexico City	1969	2002	PM10, PM2.5	126; 78 μg/m^3
			Benzen	4 ppb
			VOC	22.2 μg/m^3
		2010-2011	Bakteri ve Mantar	415; 284 CFU/m^3
Montreal	1966	2003	Mn	32 ng/m^3
Buenos Aires	1913	2002-2006	TSP	211 μg/m^3
			Fe, Zn, Cu	86; 0.08; 0.8 μg/m^3
Santiago	1975	2011	PM2.5	16.9 μg/m^3
AVRUPA				
London	1863	1996	Mantar	284 CFU/m^3
			PM2.5	892.8 μg/m^3
Barcelona	1924	2013	PM10, PM3, PM1	183; 165; 67 μg/m^3
Milan	1964	2010	UFP; PM10, PM2.5, PM1	1.3 × 10^4 adet/cm^3; 147.7;
				91.1; 36.7 μg/m^3
Italya şehirleri	1964	2006	PM10, PM2.5	217; 53 μg/m^3
Lisbon	1959	2014	PM10, PM2.5	40; 13 μg/m^3
Berlin	1902	1995	PAHs	19.7 ng/m^3
Frankfurt	1902	2013	PM10, PM2.5, PM1	77; 44; 23 μg/m^3
Paris	1900	2007	Fe	41.8%
Stockholm	1950	2000	PM10, PM2.5	390; 139 μg/m^3

(Continued)

Table 2: *Continued*

Ctiy	Metro production year	Measurement year	Polluting	Average concentration
Helsinki	1982	2004	PM2.5	53 μg/m^3
Prague	1974	2004	PM10, PM2.5, PM1	164.3; 93.9; 44.8 μg/m^3
Budapest	1894	2007	PM10; Fe	155 μg/m^3, 40%
Athens	2000	2013	PM10, PM2.5, PM1	400; 100; 40 μg/m^3
İstanbul	1910	2007 [24–27]	PM10, PM2.5	50–200; 49–181 μg/m^3
			Fe, Cu	10–28 ; 0.13–0.32 μg/m^3;

In previous studies mentioned earlier, it is seen that they have mostly compared measurement results to standard values. However, there is no study on how PM would be distributed in enclosed spaces, especially in metro, light metro, and tram systems during a global health crisis such as COVID-19.

The importance of thermal comfort is shown in studies on the increase in heat stress and changing climate in cities [10], in studies on finding monthly and annual maximum and minimum average temperature values [11], and in geostatistical methods of lead-zinc-silver mineral deposit. In the study of modeling and calculating the underground grade distribution and reserve by applying reserve parameters (density, area, thickness, grade, etc.) [12]. It is especially preferred in air pollution studies. Different approaches are applied in modeling pollution by constructing geostatistical, linear, or nonlinear models in the forward or backward direction. It is important to use emission inventory, meteorological, and topographic conditions together in layers with different methods for the spatial distribution of pollutant concentration. The methods developed in this study are based on obtaining different coefficients on the time and space scale and applying them in different layers [13]. Inverse distance weighting (IDW) was preferred due to the close and distant relationship of air studies with pollutant sources in the main theory of increasing the effect as you get closer and decreasing the effect as you move away. While the pollutant source is dirtier, the pollutant effect decreases at long distances. For this reason, the IDW method is preferred in many international studies to create spatial distribution maps [14–18].

2 Parameters affecting indoor air quality in light metro systems

2.1 Temperature (°C) and relative humidity (%)

Thermal comfort and indoor air quality are closely related. Perceived air quality changes depending on variations in the thermal conditions of interior spaces. Temperature and humidity depend on changes in the enthalpy (total energy) of air, and they change how the RT is cooled. The temperature of the respiratory mucosa of humans is between ~30 and ~32°C. While cooling the mucosal membrane to the optimum temperature and humidity ranges provides more acceptable breathing and comfort, insufficient cooling results in respiratory problems [19–21]. In field studies conducted inside buildings, it has been stated that the effects of normal temperature and humidity are negligible, and air pollutant concentrations are the main parameters at low enthalpy levels, whereas pollutant concentrations are not significantly effective at high enthalpy levels. The main parameters controlling perceived air quality are temperature and relative humidity. For indoor air quality, the optimum ranges of temperature (18–28°C) and humidity (30–70%) are reported in the ASHRAE standards. According to the ASHRAE standard 62-1989 titled "Ventilation for Acceptable Indoor Air Quality," a clean air feeding rate of 8.0 L/s (28.8 m^3/h) is recommended for transportation vehicles, waiting rooms, and platforms [10,22].

2.2 PM

PM is defined as solids, liquids, or a mixture of liquids surrounding solid particles in air. These particles may consist of both organic and inorganic substances such as dust, smoke, soot, liquid droplets, spores, bacteria, metallic compounds, elemental carbon, and inorganic ions. Some particles in the atmosphere are hygroscopic, and they absorb moisture. Organic particles include complexes that can consist of hundreds of organic compounds [23].

Particle size refers to the diameter of a particle. The classification of particles based on their diameters according to the United States Environmental Protection Agency (EPA) is shown in Table 3.

Figure 1 shows the PM concentrations reported for underground metro stations in different cities of the world listed according to measurement years.

Table 3: EPA classification of particles based on their aerodynamic diameters [30]

EPA particle size definitions:	
Highly coarse	DPa > 10 μm
Coarse	2.5 μm < DPa ≤ 10 μm
Fine	0.1 μm < DPa ≤ 2.5 μm
Ultrafine	DPa ≤ 0.1 μm

In all studies in the literature, $PM_{2.5}$ and PM_{10} values have been measured.

2.3 Aerosols

Aerosols are found both inside and outside metro cars. In addition to their negative effects on human health, aerosols also have significant direct and indirect effects on the global climate as a parameter of outside air quality. A direct effect of aerosols on the climate depends on how much they reflect or absorb solar radiation. Moreover, aerosol particles can affect the lifespan and size of clouds by acting as cloud condensation nuclei [28]. It is known that desert dust, which constitutes most of the aerosols released into the atmosphere, triggers precipitation in low clouds [29]. For these reasons, in this study, aerosol parameters depending on outside air were examined using spatial data maps.

2.4 Carbon monoxide (CO)

CO is a colorless, odorless, and tasteless gas that is formed by the incomplete combustion of carbon-containing fuels. The main source of CO in outdoor spaces is transportation. More than 70% of the release of CO in the world and 44% of

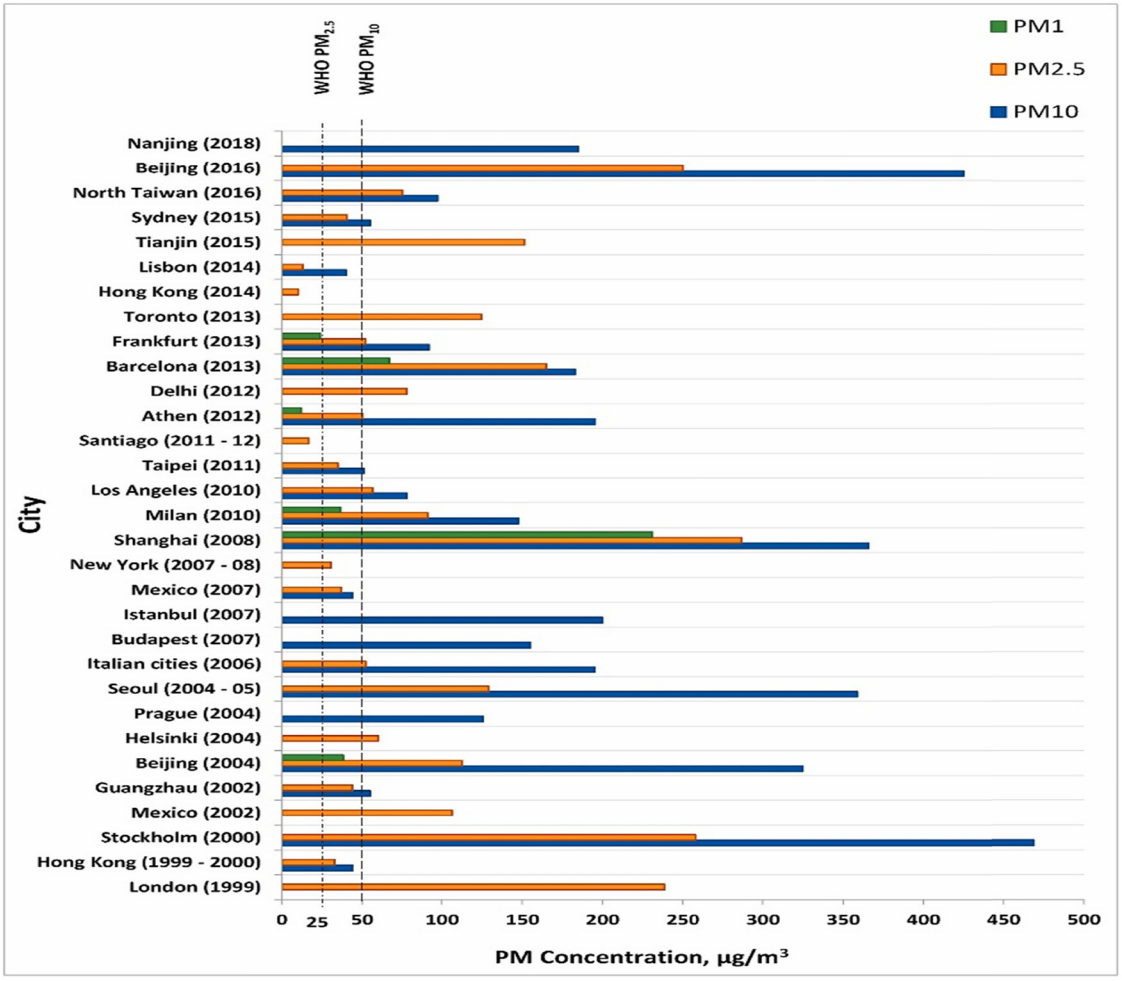

Figure 1: PM concentration measurements in different cities of the world by years [31].

Figure 2: An Antalya ANTRAY light metro train.

the release of CO in Turkey originates from the transportation sector (IPCC, 2007).

Even at low concentrations, the health effects of CO can be observed. CO enters the body via inhalation, it is not metabolized in the body, and it is removed by exhalation. Exposure to CO at low concentrations leads to fatigue even in healthy individuals, while it can result in chest pain in individuals with cardiovascular problems. Exposure to higher concentrations can reduce the sensation of sight and the ability to communicate and cause headaches, dizziness, imbalance, and nausea. Fatal outcomes can be seen at high concentrations [10,22].

3 Materials and methods

In this study, temperature, humidity, and PM values were measured and automatically recorded on a Fluke 983 device at 16 stations with the highest human traffic in the light metro system of the Antalya Metropolitan Municipality (Figure 2) with a total of 25 stations (Figure 3). Because the number of measurements was too high, only some of the measurements made in the light metro system (ANTRAY) are presented in Table 4.

The technical properties of the air conditioning setup used in the ANTRAY light metro system are not presented as the setup was not operated during the COVID-19 period.

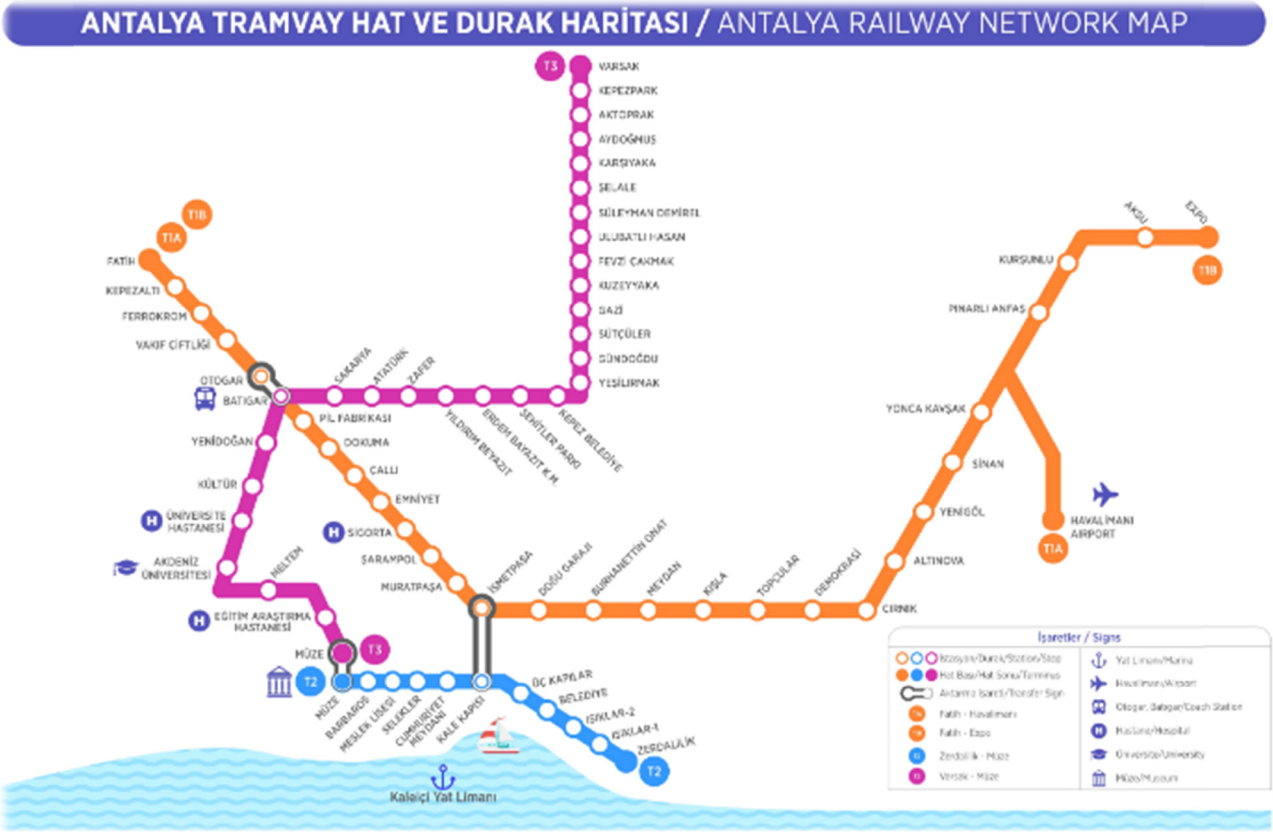

Figure 3: Light metro and tram lines and stops/platforms in Antalya, Turkey.

Table 4: ANTRAY air quality parameter measurements

Light metro stop name	Indoor air particles substance, temperature, and humidity values								Outside air particles matter
	0.3 µm	0.5 µm	1.0 µm	2.0 µm	5.0 µm	10 µm	Sıcaklık (°C)	Bağıl Nem (%)	PM 10 µm
Ferro krom	198,566	17,311	1,102	400	46	17	25	54	26.90
Kepezaltı	188,568	15,172	768	225	17	6	25	54	21.01
Fatih	186,368	15,225	1,150	508	40	9	25	53	22.10
Vakıf Çitliği	169,479	12,200	634	203	11	4	25	55	29.30
Otogar	166,947	12,197	762	276	25	10	25	55	36.89
Pil fabrikası	160,509	11,005	591	192	14	6	26	53	38.86
Dokuma	155,137	10,294	454	113	5	3	26	53	34.18
Callı	186,077	17,061	2,503	1,304	110	30	30	49	28.48
Emniyet	154,479	10,200	659	235	23	7	23	52	26.29
Sigorta	166,716	13,455	1,177	464	41	8	25	52	25.88
Şarampol	147,721	9,739	502	131	9	3	26	50	26.71
Muratpaşa	158,375	11,034	692	202	10	3	26	49	29.12
İsmetpaşa	154,628	10,377	544	159	6	4	26	49	30.54
Doğu garajı	148,780	9,791	467	89	8	2	26	50	29.29
B.Onat	168,258	12,903	681	192	7	3	27	48	25.55
Meydan	163,719	12,094	570	126	5	2	26	50	21.69
Kışla	215,059	25,395	2,905	1,315	13	26	26	46	22.56
Topcular	204,064	18,290	1,112	280	17	9	26	50	25.59
Demokrasi	229,764	23,193	1,327	325	34	12	26	48	25.47
Cırnık	254,596	30,978	2,321	738	47	8	25	47	27.22
Altınova	233,572	24,077	1,389	374	13	2	25	47	30.82
Yenigöl	234,453	23,726	1,418	370	20	5	27	46	33.62
Sinan	237,791	24,237	1,289	303	12	3	26	45	40.55
Yonca kavşağı	217,924	19,044	694	65	2	1	26	45	50.40
Dış hatlar	205,754	16,951	596	62	0	0	26	45	22.38

Measurements were made inside and outside metro cars at 16 stations with the highest human traffic from the Fatih station to the Meydan station. Each station was numbered. For example, the Fatih station was coded S1, while the Meydan station was coded S16. The hand-held Fluke 983 PM measurement device that was used in the study is shown in Figure 4.

Figure 4: Fluke 983 PM measurement device.

Some of the temperature, relative humidity, and PM measurement values recorded on 8 February, 22 February, and 8 March 2021, which corresponded to the active phase of the COVID-19 pandemic, are presented in Table 4.

The accuracy and calibration of the measuring devices were made by the relevant companies. In the study, daily measurements were taken three times: in the morning, at noon and in the evening. In each measurement, measurements were taken from close to the ground in the subway, again from 1 m above the ground and from 1.5 m above the ground.

Using the temperature, relative humidity, and PM (0.3, 0.5, 1, 5, and 10 µm) measurement results for indoor (in metro cars) and outside (stations) air quality parameters which are shown in Table 4, as well as aerosol, CO, formaldehyde, normalized difference vegetation index (NDVI), NO_2, and SO_2 values, spatial maps were created in the geographic information system (GIS) using the IDW method. The maps were produced in the order given below, and each map was examined in the context of the indoor air quality analyses. Since the study was conducted during the Covid-19 pandemic, there is no information on the number of passengers.

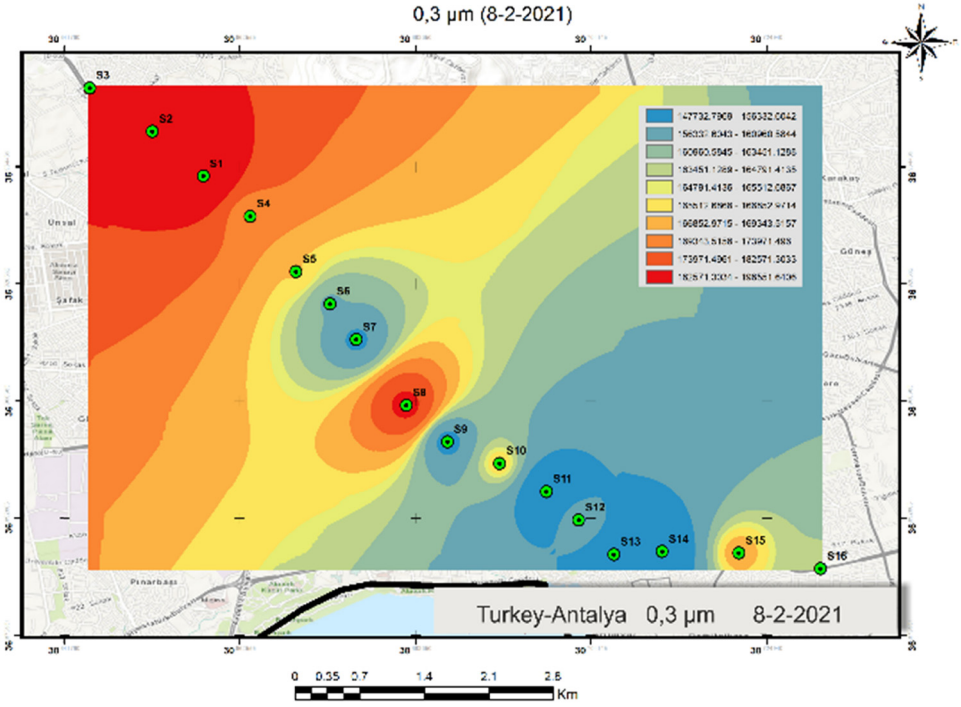

Figure 5: Spatial map of $PM_{0.3}$ based on measurements on 8 February 2021 (indoor).

In Figure 5, the dark red zones show the very high concentrations of $PM_{0.3}$ at S1, S2, and S3 among the 16 stations where the measurements were made on 8 February 2021. The lowest $PM_{0.3}$ concentrations, shown in dark blue, were measured at S7, S11, S13, and S14.

On Figure 6, the dark red zones show the very high concentrations of $PM_{0.3}$ at S1, S2, S3, S8, and S9 among the 16 stations where the measurements were made on 22 February 2021. The lowest $PM_{0.3}$ concentrations, shown in dark blue, were measured at S13, S14, S15, and S16.

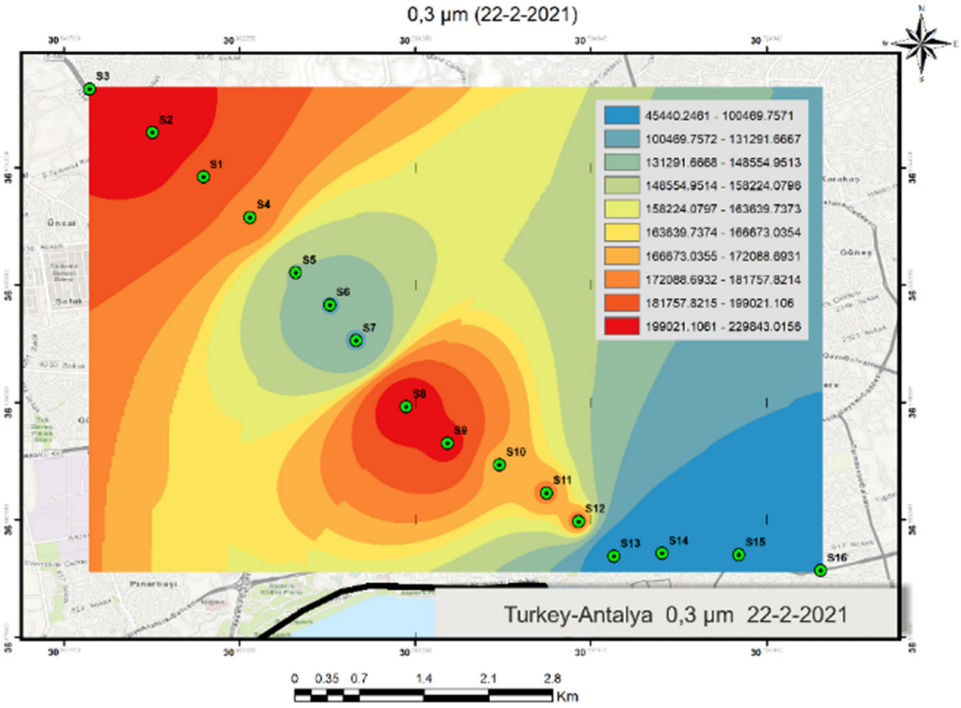

Figure 6: Spatial map of $PM_{0.3}$ based on measurements on 22 February 2021 (indoor).

On Figure 7, the dark red zones show the very high concentrations of $PM_{0.3}$ at S1, S2, S3, S4, S5, and S6 among the 16 stations where the measurements were made on 8 March 2021. The lowest $PM_{0.3}$ concentrations, shown in dark blue, were measured at S9, S10, S11, and S12.

According to Maps 1, 2, and 3, S1, S2, and S3 had very high concentrations of $PM_{0.3}$ on all measurement days. Among these stations, S1 was the station where the light metro line started, and it had a high traffic of people both inside and outside the metro cars. In addition, considering that the area was a crowded area where large numbers of working people would be present, it may have been the first point of the spread of COVID-19 through the light metro system. The lowest $PM_{0.3}$ concentrations were at S13 and S14 on all measurement days. These were the Doğu Garajı and Burhanettin Onat stations, which were located right after the point where the light metro traffic connected to other lines, meaning that passenger traffic would be less.

According to these results, an infrared thermometer could be used at the entrance of the stations to prevent those with a fever from using the metro.

In Figure 8, the dark red zones show the very high concentrations of $PM_{0.5}$ at S1, S2, S3, and S8 among the 16 stations where the measurements were made on 8 February 2021. The lowest $PM_{0.5}$ concentrations, shown in dark blue, were measured at S11, S12, S13, and S14, which included the Doğu Garajı and Burhanettin Onat stations where lower rates of passenger traffic would be found.

In Figure 9, the dark red zones show the very high concentrations of $PM_{0.5}$ at S1 and S8 among the 16 stations where the measurements were made on 22 February 2021. The lowest $PM_{0.5}$ concentrations, shown in dark blue, were measured at S13, S14, S15, and S16, which included the Doğu Garajı and Burhanettin Onat stations where lower rates of passenger traffic would be found.

In Figure 10, the dark red zones show the very high concentrations of $PM_{0.5}$ at S1, S2, S4, S5, and S6 among the 16 stations where the measurements were made on 8 March 2021. The lowest $PM_{0.5}$ concentrations, shown in dark blue, were measured at S9, S10, S11, and S12.

According to Figures 8–10, S2 and S8 had very high concentrations of $PM_{0.5}$ on all measurement days. Among these stations, S1 was the station where the light metro line started, and it had a high traffic of people both inside and outside the metro cars. In addition, considering that the area was a crowded area where large numbers of working people would be present, it may have been the first point of the spread of COVID-19 through the light metro system. The lowest $PM_{0.5}$ concentrations were at S13 and S14 on all measurement days. These were the Emniyet and Sigorta stations.

According to these results, an infrared thermometer could be used at the entrance of the stations to prevent those with a fever from using the metro.

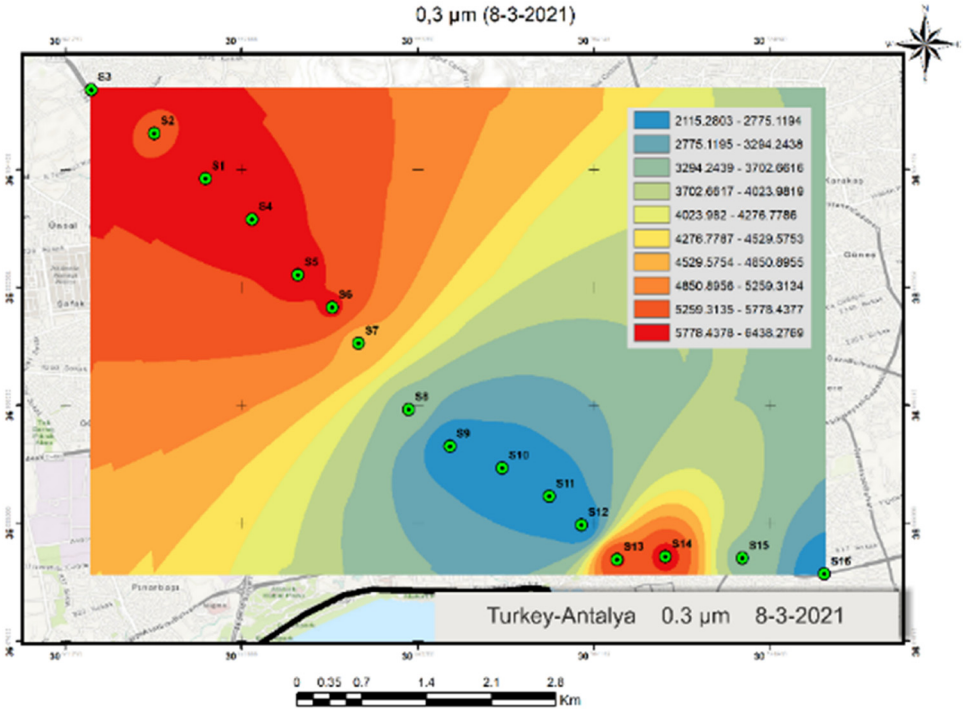

Figure 7: Spatial map of $PM_{0.3}$ based on measurements on 8 March 2021 (indoor).

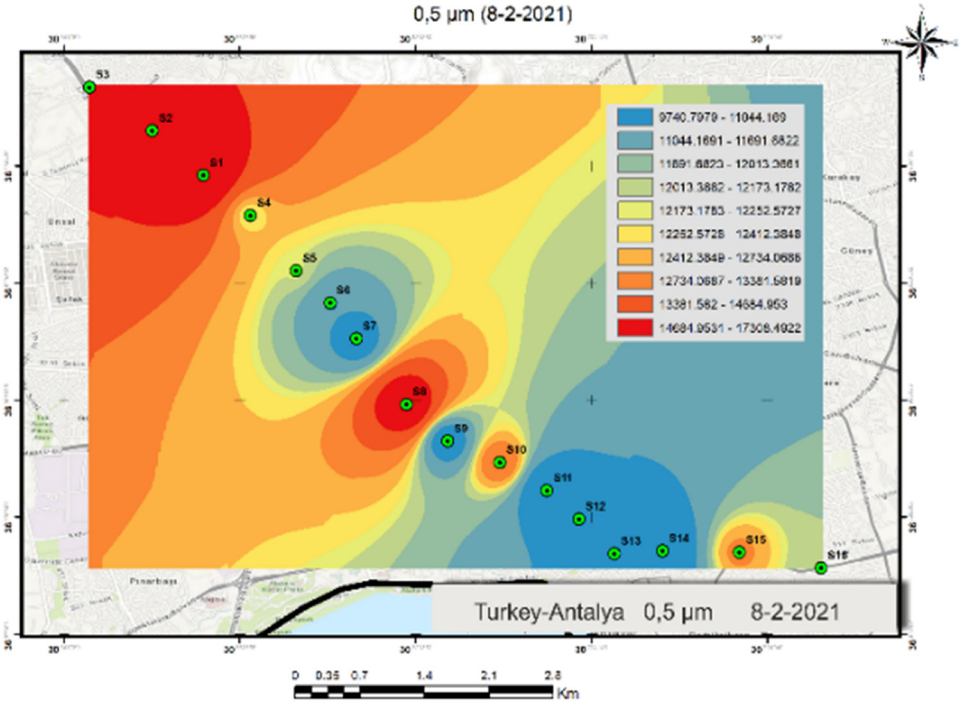

Figure 8: Spatial map of $PM_{0.5}$ based on measurements on 8 February 2021 (indoor).

In Figure 11, the dark red zones show the very high relative humidity values at S6 among the 16 stations where the measurements were made on 8 February 2021. The lowest relative humidity values, shown in dark blue, were measured at S9, which was the Çallı station.

In Figure 12, the dark red zones show the very high relative humidity values at S15 among the 16 stations where the measurements were made on 22 February 2021. The lowest relative humidity values, shown in dark blue, were measured at S4.

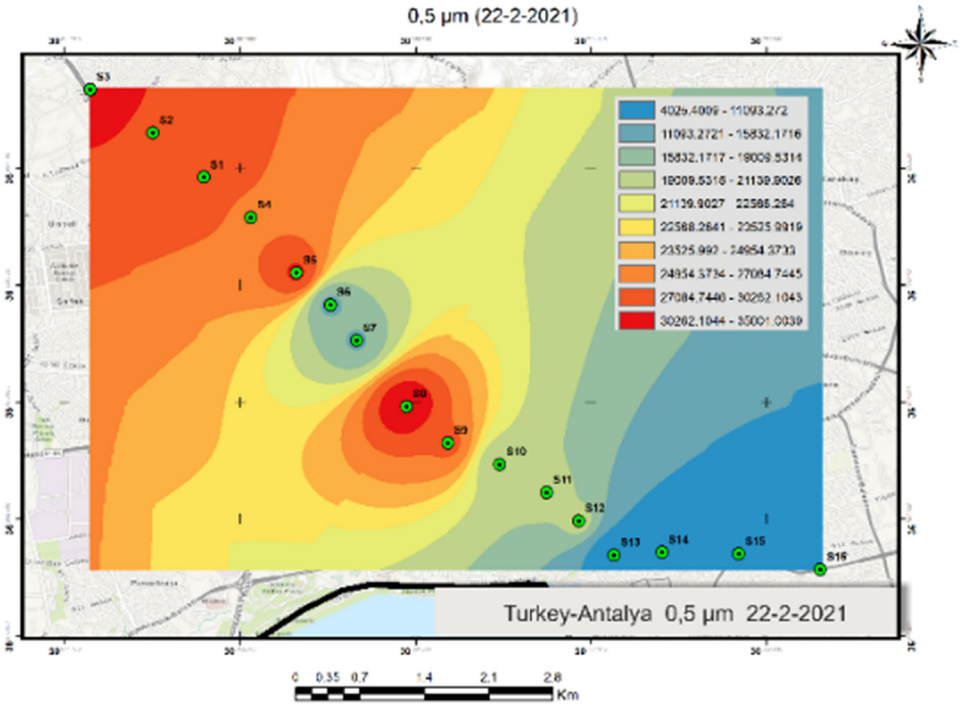

Figure 9: Spatial map of $PM_{0.5}$ based on measurements on 22 February 2021 (indoor).

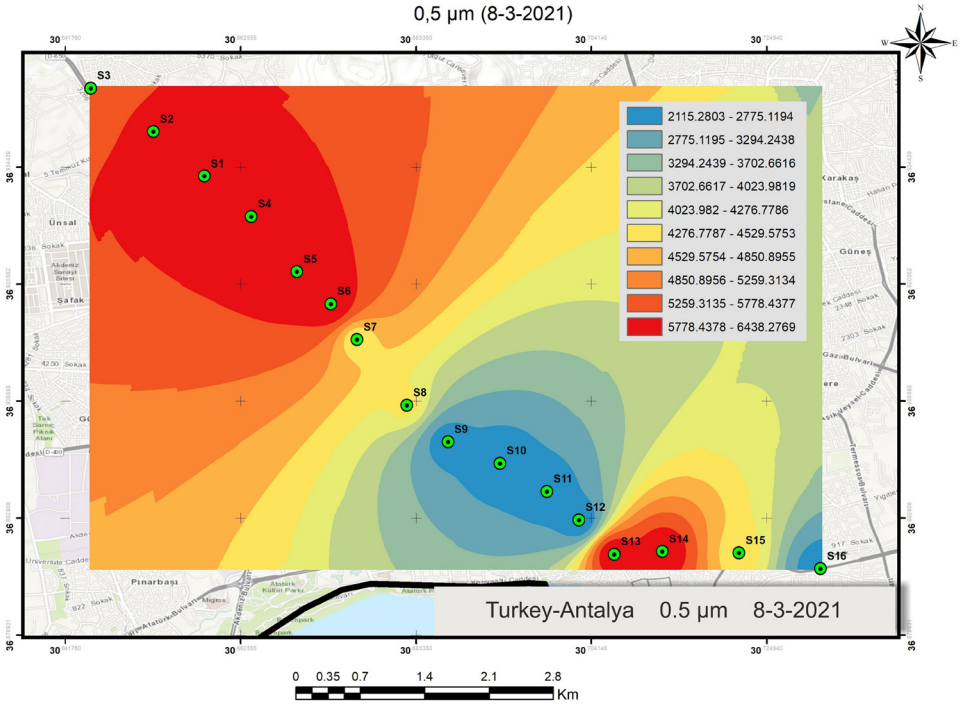

Figure 10: Spatial map of $PM_{0.5}$ based on measurements on 8 March 2021 (indoor).

In Figure 13, the dark red zones show the very high relative humidity values at S9, S10, S11, and S12 among the 16 stations where the measurements were made on 8 March 2021. Relative humidity could be high in these areas due to evaporation as they were close to the underground stream named Kırkgöz, which supplies the drinking water

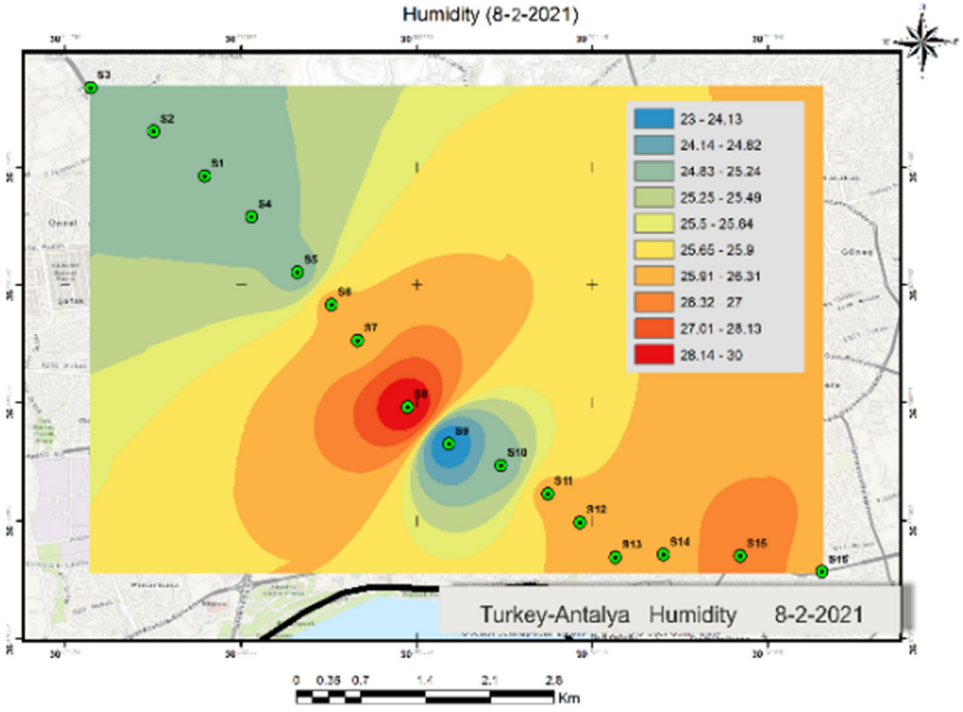

Figure 11: Spatial map of relative humidity (%) based on measurements on 8 February 2021 (indoor).

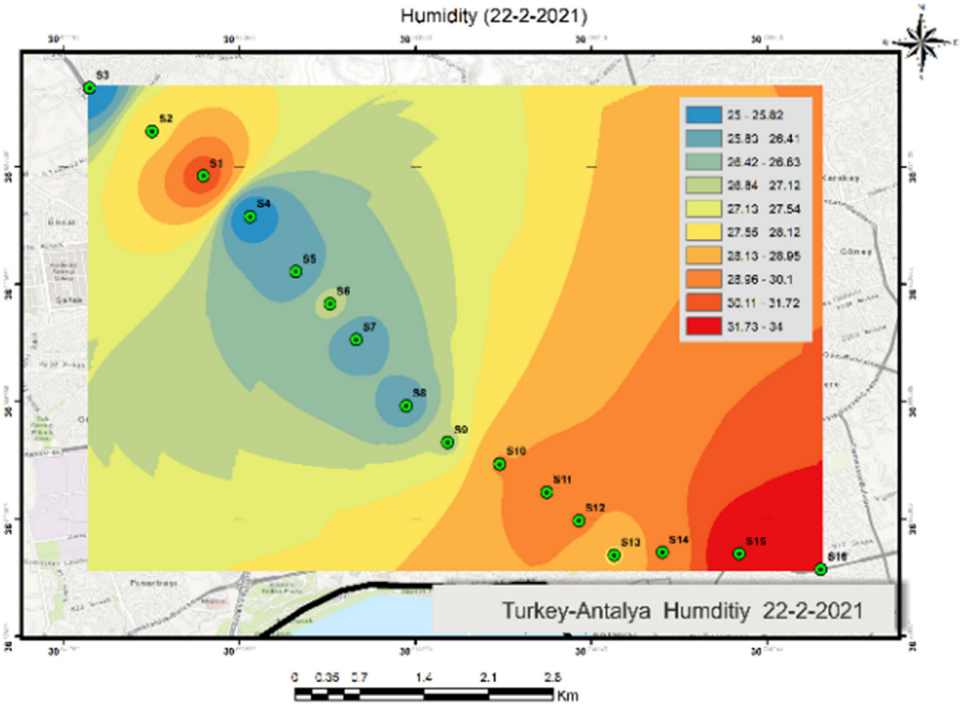

Figure 12: Spatial map of relative humidity (%) based on measurements on 22 February 2021 (indoor).

of Antalya, and the hydroelectric power plant, which is fed by Kırkgöz through canals. The lowest relative humidity values, shown in dark blue, were measured at S1, S2, and S3.

According to Figures 11–13, the relative humidity values in the area were not similar on different measurement days.

In Figure 14, the dark red zones show the highest outside temperature values at S8 among the 16 stations where the measurements were made on 8 February 2021. The lowest temperature values, shown in light blue, were measured at S9.

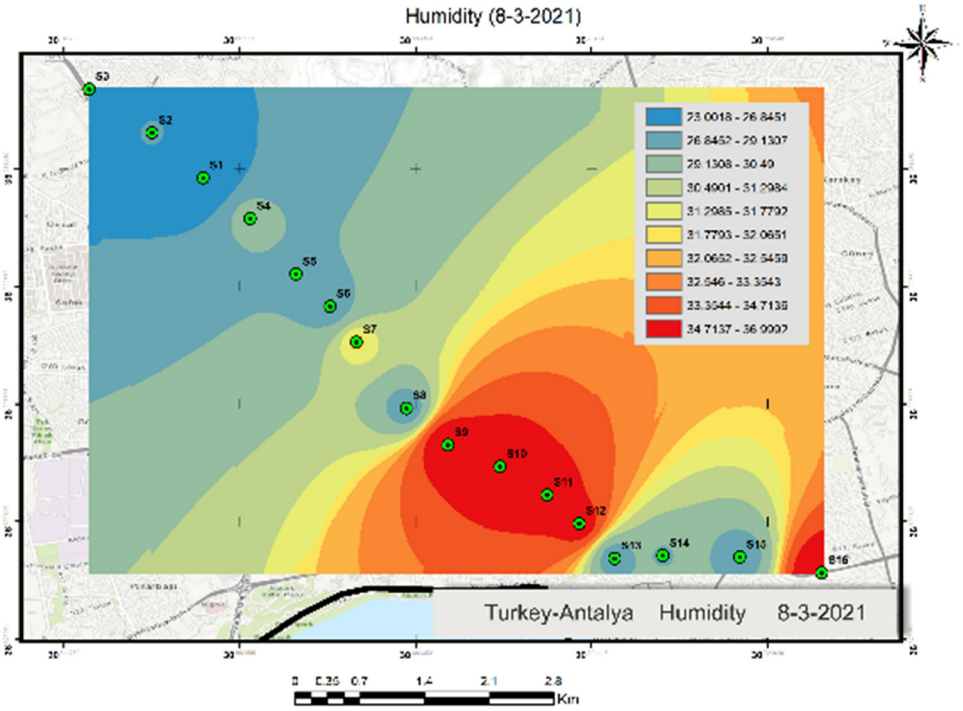

Figure 13: Spatial map of relative humidity (%) based on measurements on 8 March 2021 (indoor).

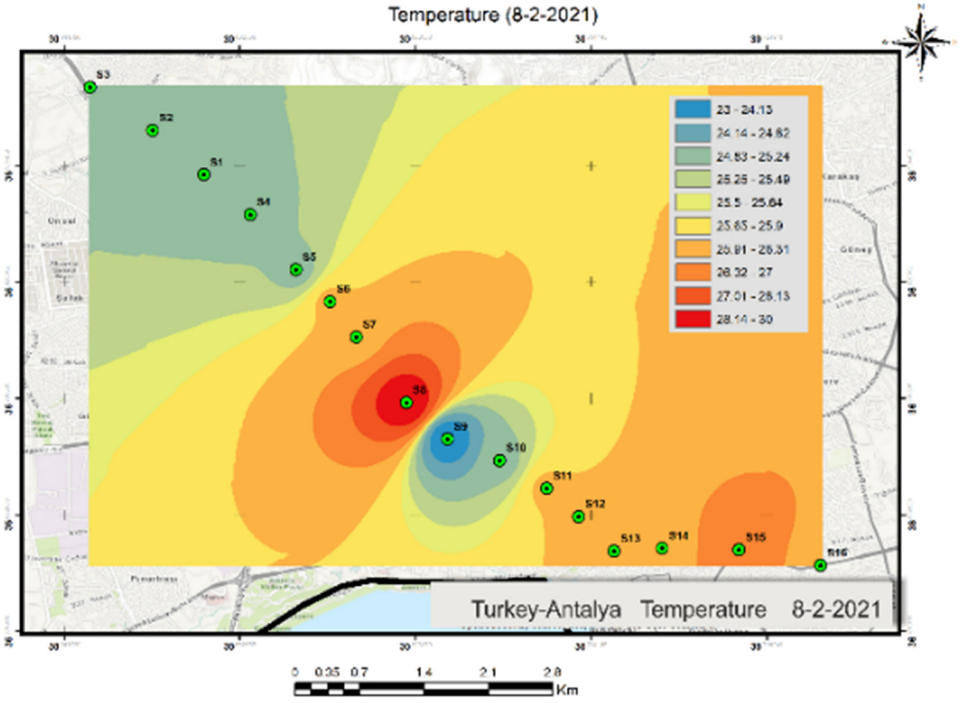

Figure 14: Spatial map of outside temperature (°C) based on measurements on 8 February 2021.

In Figure 15, the dark red zones show the highest outside temperature values at S6 and S12 among the 16 stations where the measurements were made on 22 February 2021. The lowest temperature values were measured at S13 and S14.

In Figure 16, the dark red zones show the highest outside temperature values at S1 among the 16 stations where the measurements were made on 8 March 2021. The lowest temperature values, shown in blue, were measured at S9.

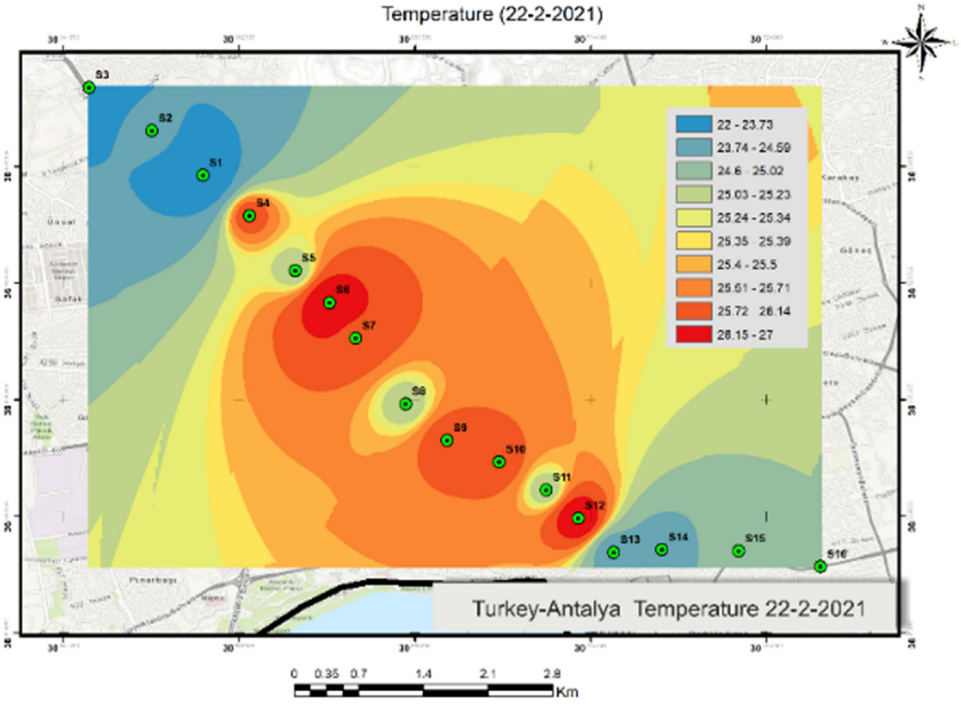

Figure 15: Spatial map of outside temperature (°C) based on measurements on 22 February 2021.

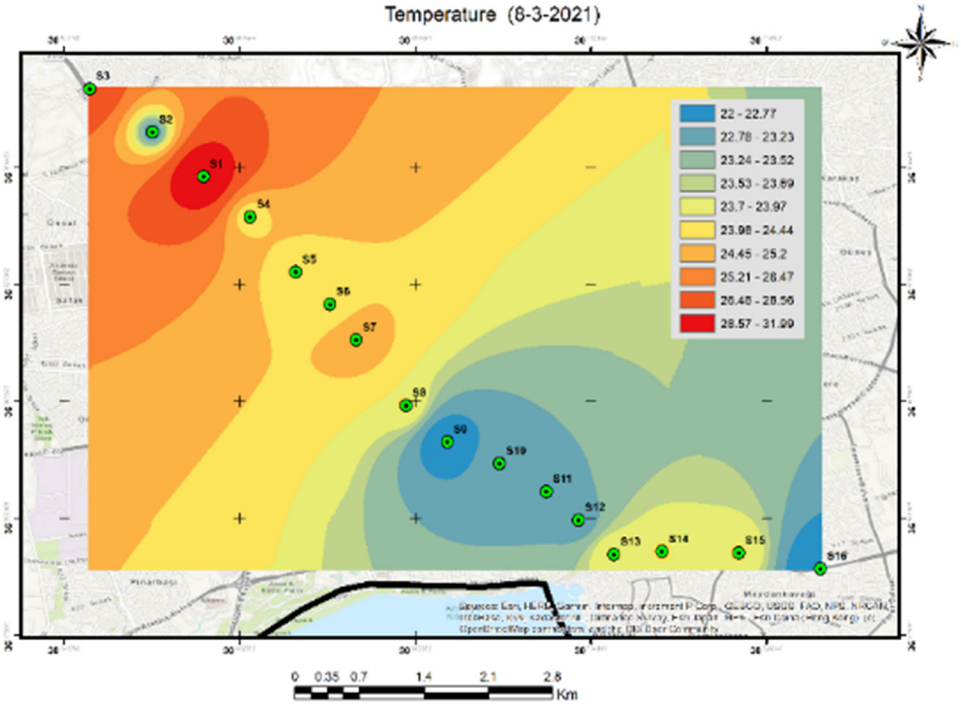

Figure 16: Spatial map of outside temperature (°C) based on measurements on 8 March 2021.

According to Figures 14–16, S8, S6, S12, and S1 had the highest outside temperature measurements. No apparent relationship could be found between these temperature values and their spatial distributions. On the other hand, S9, S13, S14, and S9 had the lowest outside temperatures, with the lowest at S9, which was the Çallı station.

As shown in Figure 17, which shows the CO measurements made on 8 February (a), 22 February (b), and 8 March 2021 (c), the CO concentrations between S4 and S16 were very low, while the CO concentrations between S3 and S4 (Fatih and Vakıf Çiftliği stations) were very high. The reason for the high concentrations of CO in this area may be the industrial zone of Antalya and the ferrochromium factory at the location. Other spatial maps also showed that the areas with high CO concentrations also had high $PM_{0.3}$ and $PM_{0.5}$ concentrations.

Figure 18 shows the measurements of aerosols, which considerably affect air quality, made on 8 February (a), 22 February (b), and 8 March 2021 (c). The aerosol concentrations between S7 and S16 were very high. This was attributed to the high traffic of people in these areas due to their proximity to the city center.

Figure 19 shows the spatial maps of the NDVI values measured on 8 February (a), 22 February (b), and 8 March (c). It is seen that the area between S7 and S16 had a low amount of vegetation, and this was attributed to the proximity of the area to the city center. On the other hand, in seven areas between S3 and S7, a relatively higher amount of vegetation was observed. This result may be explained by the presence of an olive grove in the area consisting of several olive trees.

4 Discussion and conclusion

The following results were obtained based on the measurements that were made with difficulty in Antalya in Turkey on 8 February, 22 February, and 8 March 2021, when mask and social distancing rules were in place due to the COVID-19 pandemic.

a) $PM_{0.3}$ analysis results:

According to Figures 5–7, S1, S2, and S3 had very high concentrations of $PM_{0.3}$ on all measurement days. Among these stations, S1 was the station where the light metro line started, and it had a high traffic of people both inside and outside the metro cars. In addition, considering that the area was a crowded area where large numbers of working people would be present, it may have been the first point of the spread of COVID-19 through the light metro system. The lowest $PM_{0.3}$ concentrations were at S13 and S14 on all measurement days. These were the Doğu Garajı and Burhanettin Onat stations, which were located right after the point

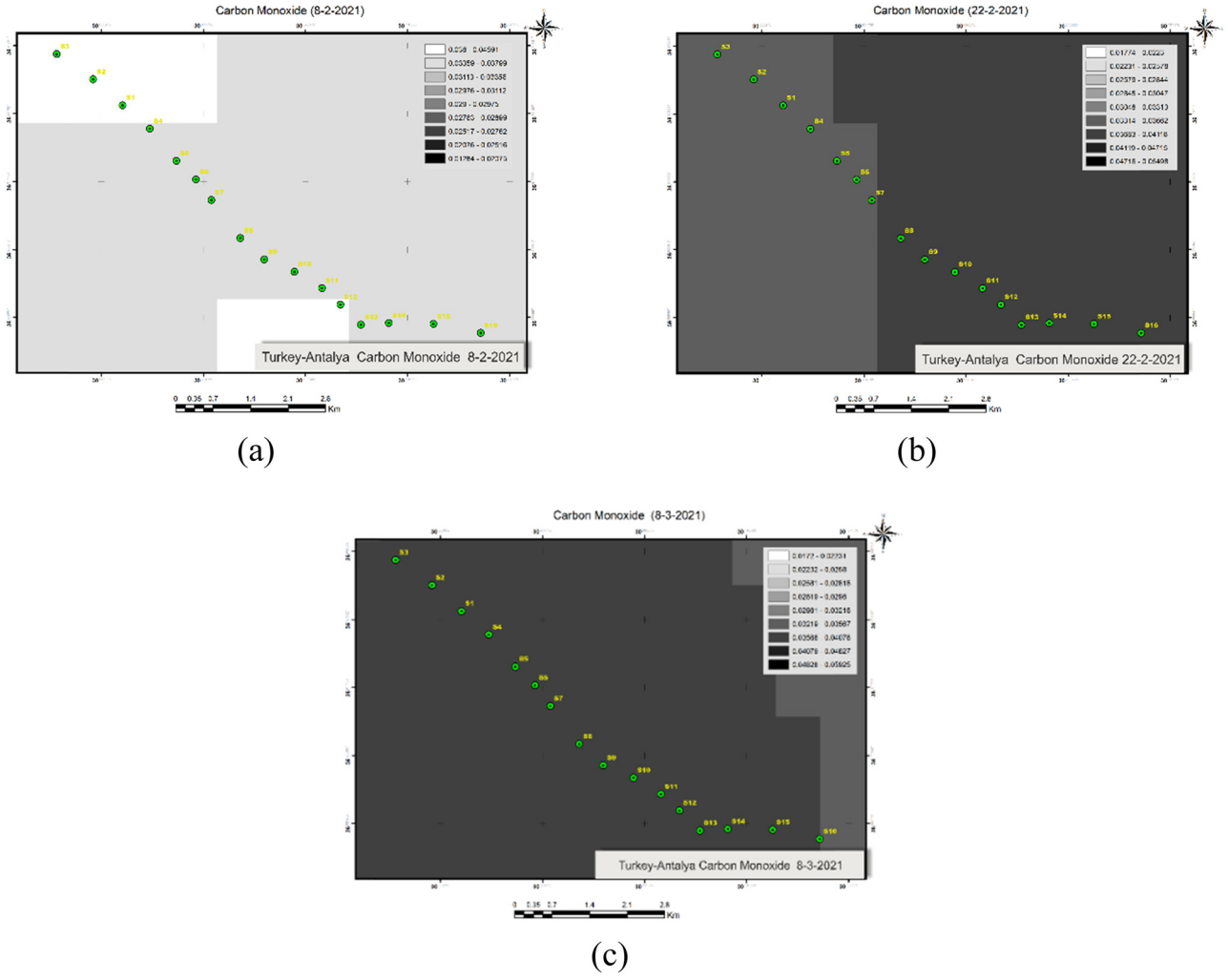

Figure 17: Spatial maps of CO on 8 February (a), 22 February (b), and 8 March 2021 (c).

where the light metro traffic connected to other lines, meaning that passenger traffic would be less.

b) $PM_{0.5}$ analysis results:

According to Figures 8–10, S2 and S8 had very high concentrations of $PM_{0.5}$ on all measurement days. Among these stations, S1 was the station where the light metro line started, and it had a high traffic of people both inside and outside the metro cars. In addition, considering that the area was a crowded area where large numbers of working people would be present, it may have been the first point of the spread of COVID-19 through the light metro system. The lowest $PM_{0.5}$ concentrations were at S13 and S14 on all measurement days. These were the Emniyet and Sigorta stations.

c) Outside temperature (°C) analysis results:

According to Figures 14–16, S8, S6, S12, and S1 had the highest outside temperature measurements. No apparent relationship could be found between these temperature values and their spatial distributions. On the other hand, S9, S13, S14, and S9 had the lowest outside temperatures, with the lowest at S9, which was the Çallı station. The spatial maps also did not show a meaningful relationship between outside temperature and $PM_{0.3}$ or $PM_{0.5}$ values.

d) Relative humidity (%) analysis results:

According to Figures 11–13, the relative humidity values in the area were not similar on different measurement days.

e) CO analysis results:

As shown in Figure 17(a)–(c), the CO concentrations between S4 and S16 were very low, while the CO concentrations between S3 and S4 (Fatih and Vakıf Çiftliği stations) were very high. The reason for the high concentrations of CO in this area may be the industrial zone of Antalya and the ferrochromium factory at the location. Other spatial maps also showed that the areas with high CO concentrations also had high

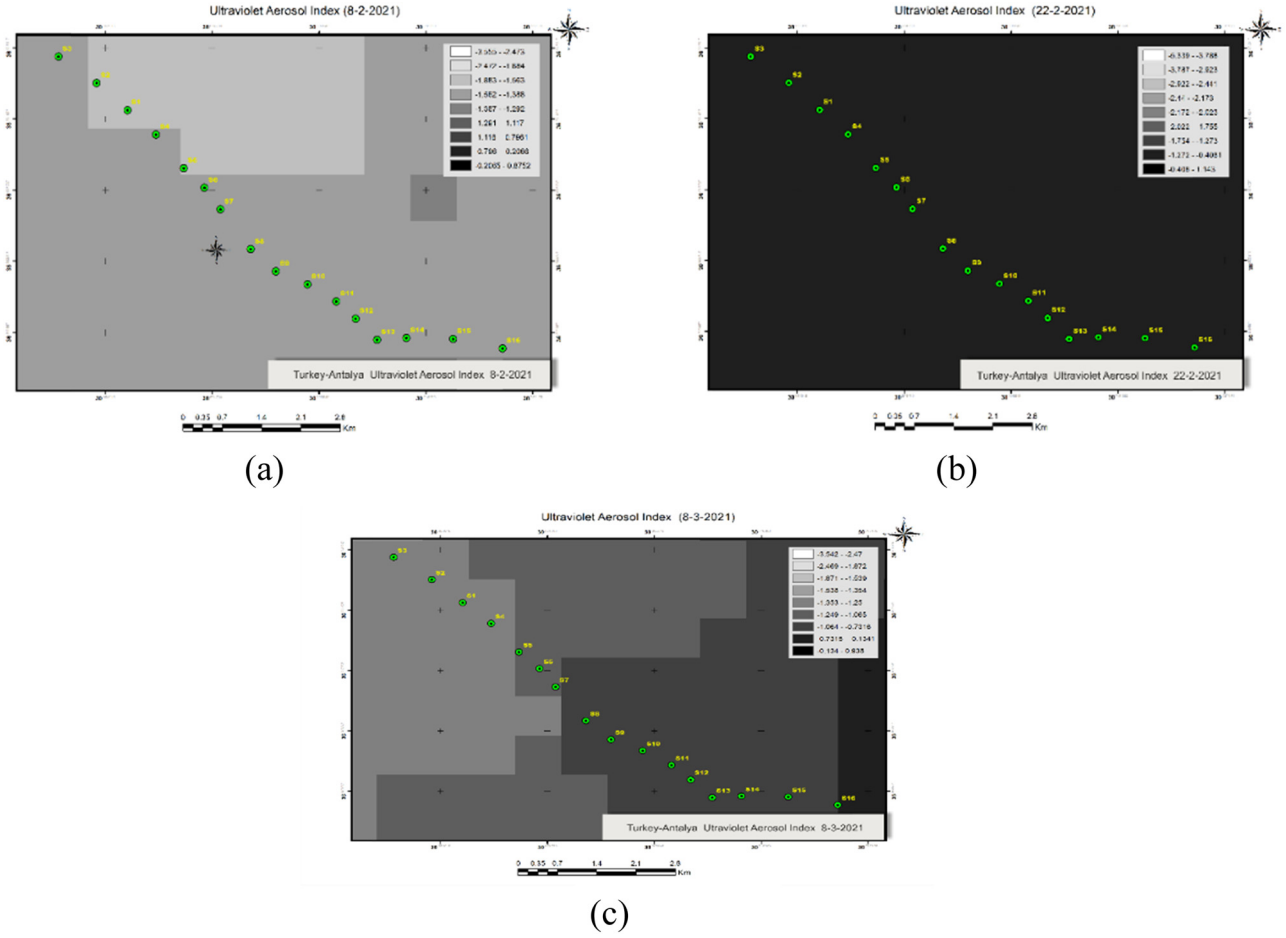

Figure 18: Spatial maps of aerosols on 8 February (a), 22 February (b), and 8 March 2021 (c).

$PM_{0.3}$ and $PM_{0.5}$ concentrations, which could indicate a relationship.

f) Aerosol analysis results:

As shown in Figure 18(a)–(c), showing the measurements of aerosols, which considerably affect air quality, the aerosol concentrations between S7 and S16 were very high. This was attributed to the high traffic of people in these areas due to their proximity to the city center. Other spatial maps also showed increased $PM_{0.3}$ and $PM_{0.5}$ concentrations at these locations, indicating a relationship between aerosol and PM concentrations.

g) NDVI analysis results:

As shown in Figure 19, showing the spatial maps of NDVI values, the area between S7 and S16 had a low amount of vegetation, and this was attributed to the proximity of the area to the city center. On the other hand, in seven areas between S3 and S7, a relatively higher amount of vegetation was observed. This result may be explained by the presence of an olive grove in the area consisting of several olive trees. Moreover, in areas with low CO concentrations, vegetation was scarcer according to the NDVI values, and $PM_{0.3}$ and $PM_{0.5}$ concentrations were higher. This suggested a relationship among NDVI, CO, $PM_{0.3}$, and $PM_{0.5}$ values. It is seen that without conducting statistical analyses, the relationships among indoor air quality parameters can be observed using spatial maps.

According to the results of this study, it is recommended to use an infrared thermometer at the entrance of metro, tram, and train stations to prevent those with a fever from using these vehicles.

Metro systems are among the areas used by a large proportion of the population, where the comfort and health of passengers are affected by air quality parameters. Studies on air quality allow us to analyze human exposure to pollutants and calculate indoor air quality parameters, which can then be used to identify health risks and take precautions to protect public health. Such studies can be utilized as important tools to develop effective policies for reducing human exposure to aerosols in trams, metro, light rail, and train transportation systems.

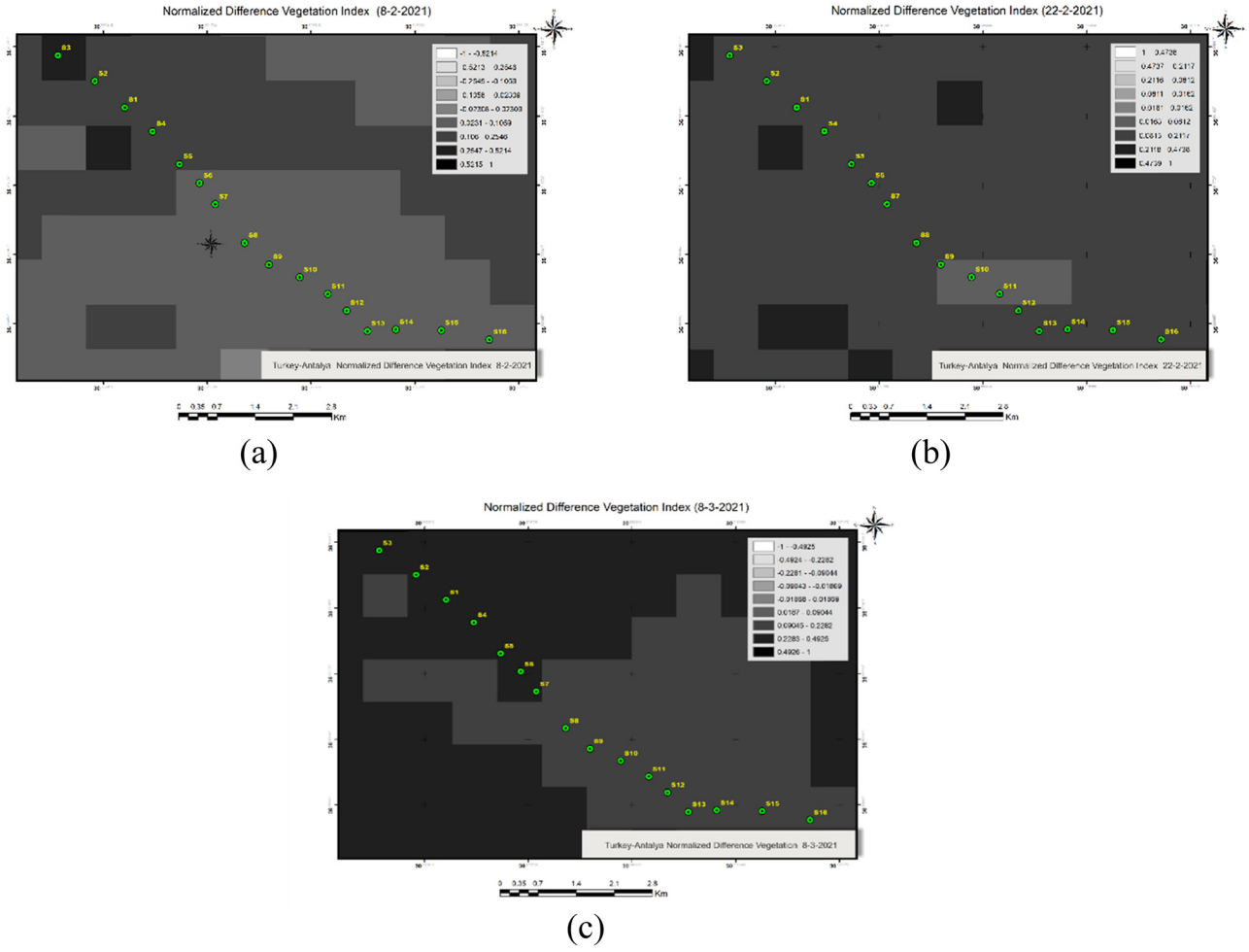

Figure 19: Spatial maps of NDVI on 8 February (a), 22 February (b), and 8 March 2021 (c).

The negative effects of PM, which is among indoor quality parameters, can be reduced in metro systems. The main issue here is to determine how to lower the PM concentrations in systems that involve the operation of metal wheels on metal rails. To reduce the concentrations of PM originating from the movement of the vehicle on the rails for older trains and metro systems, modifications such as automated brake systems, rubber tires, and air conditioning systems can be recommended. The usage of automated brake systems and rubber tires will not only reduce the concentrations of PM but also lower the levels of noise and sound that the passengers are exposed to. The implementation of these modifications in older metro systems might not always be economically and technologically viable. Using high-performance air conditioning systems is a highly effective method of eliminating PM accumulation. However, as seen in the example used in this study, in a global public health problem like the COVID-19 pandemic, the air conditioning systems of metro systems may be turned off to minimize the spread of viruses. Because these systems not only lower the PM concentrations inside metro cars but also provide the passengers with thermal comfort by providing optimal temperature and humidity conditions, it is recommended to use HEPA filters in air conditioning equipment used for metro systems. These filters can also be used in older transportation systems by modifying or replacing their existing air conditioning equipment. The greatest disadvantage of these systems is that they consume a lot of energy. Officials are recommended to ensure that the areas where dust can accumulate at locations where trains are maintained and repaired are cleaned regularly, the cleaning of trains, stations, and platforms, in general, is not overlooked, and PM concentrations at certain locations are regularly measured using appropriate devices.

It is recommended that field studies be carried out to investigate the effects of thermal parameters on perceived indoor air quality in terms of the exposure of passengers to various air pollutants in metro and tram cars, as well as

underground stations and platforms. In addition, in underground stations, more attention should be paid to mechanical ventilation systems, including air filtering systems, by using an integrated building management system. These measures can improve the general indoor air quality in metro systems.

Previous studies on indoor air quality in metro systems have mostly compared field measurements to standard values. However, there is no study on how PM would be distributed in enclosed spaces, especially in metro, light metro, and tram systems during a global health crisis such as COVID-19. This is why it is believed that this study is unique. Furthermore, by taking the results of this study as a reference, it will be possible to create spatial maps of various indoor air quality parameters such as temperature, humidity, PM, and VOC for other areas where air quality is important, including residential buildings, hospitals, and shopping malls.

Considering that PM1 (1 μm) and smaller particles are small enough to enter the bloodstream of humans through the alveoli in their lungs, this study was planned to measure the concentrations of $PM_{0.3}$ (0.3 μm) and $PM_{0.5}$ (0.5 μm), which are smaller than PM1, as a pioneering study to investigate their effects on human health.

Funding information: The author states no funding.

Author contributions: The author confirms sole responsibility for the following: study conception and design, data collection, analysis and interpretation of results, and manuscript preparation.

Conflict of interest: The authors declare no conflict of interest.

Ethical approval: The conducted research is not related to either human or animal use.

Data availability statement: The data used to support the findings of this study are available from the corresponding author upon request.

References

[1] Nieuwenhuijsen M, Gómez-Perales J, Colvile R. Levels of particulate air pollution, its elemental composition, determinants and health effects in metro systems. Atmos Environ. 2007;41:7995–8006. doi: 10.1016/j.atmosenv.2007.08.002.

[2] Xu B, Hao J. Air quality inside subway metro indoor environment worldwide: A review. Environ Int. 2017;107:33–46.

[3] Mammi-Galani E, Eleftheriadis K, Mendes L, Lazaridis M. Exposure and dose to particulate matter inside the subway system of Athens, Greece. Air Qual Atmos Health. 2017;10(10):1015–28. doi: 10.1007/s11869-017-0490-z.

[4] Abanoz MS. İstanbul'da metrolarda iç hava kalitesine havalandırma sistemine etkisi. İstanbul Üniversitesi Cerrahpaşa Lisansüstü Eğitim Enstitüsü Çevre Mühendisliği anabilimdalı. İstanbul, TürkiyeHaziran: 2019.

[5] Onat B. Metro istasyonları ile metro ve şehirlerarası tren vagonlarında iç hava kalitesi. Teskon 2015 İç Hava Kalitesi Semineri. İzmir, Türkiye; 2015.

[6] Çoşgun A, Okuyan C. Antalya ilinde hafif raylı metro sisteminde partiküller maddelerin iç hava kalitesine etkisinin araştırılması ve modellenmesi. 1. Ulusal İklimlendirme Soğutma Eğitimi Sempozyumu. Balıkesir, Türkiye: 2012.

[7] Onat B, Uzun B, Akın Ö, Şahin AÜ. Ulaşım araçları içinde ve dış ortamda siyah karbon ve partikül madde maruziyeti. Teskon 2017/İç Hava Kalitesi Sempozyumu. İzmir, Türkiye; 2017.

[8] Korukcu MÖ. Otomobil kabininde termal parametrelerin ve iç hava kalitesinin değişiminin deneysel ölçümlerle incelenmesi. Doktora tezi, Uludağ Üniversitesi Fen Bilimleri Enstitüsü. Bursa, Türkiye: 2020.

[9] MHSTŞ. Metro Havalandırma Sistemleri Teknik Şartname. İstanbul, Türkiye: 2018.

[10] Tağıl Ş, Ersayın K. Balıkesir ilinde dış ortam termal konfor değerlendirmesi. J Int Soc Res. 2015;8(41):747–55.

[11] Tuncer K, Yılmaz E. Muğla ilinin aylık ortalama maksimum ve minimum hava sıcaklığı dağılışının ıdw yöntemiyle coğrafi bilgi sistemleri (cbs) ortamında haritalanması ve analizi. Akademi Sosyal Bilimler Dergisi. 2023;10(28):29–51.

[12] Günaydın O. Balıkesir/Balya Hastanetepe bölgesi kurşun-çinko-gümüş yeraltı ocağı rezervinin jeoistatistik yöntemlerle değerlendirilmesi. Konya Teknik Üniversitesi, Yüksek Lisans Tezi; 2019.

[13] Toros H, Bağış S, Gemici Z. Ankara'da hava kirliliği mekânsal dağılımının modellenmesi. Ulusal Çevre Bilimleri Araştırma Dergisi. 2018;1(1):20–53.

[14] Rahman MH, Agarwal S, Sharma S, Suresh R, Kundu S, Vranckx S, et al. High-resolution mapping of air pollution in delhi using Detrended Kriging Model. Environ Model Assess. 2023;28(1):39–54.

[15] Gogeri I, Gouda KC, Aruna ST. Spatio-temporal analysis of air pollution dynamics over Bangalore city during the second wave of COVID-19. Nat Hazards Res. 2023;1–65.

[16] Nasehi S, Yavari A, Salehi E. Investigating the spatial distribution of land surface temperature as related to air pollution level in Tehran metropolis. Pollution. 2023;9(1):1–14.

[17] Tang T, Fan H, Sun Q, Zhao W. Spatial and temporal analysis of daily measurements of PM2.5 Air Pollution in Beijing, China. J Geogr. 2023;11(1):1–42.

[18] Račić N, Malvić T. Relation between air and soil pollution based on statistical analysis and interpolation of Nickel (Ni) and Lead (Pb): Case study of Zagreb, Croatia. Min Miner Depos. 2023;17(2):112–20.

[19] Fadden MER. Respiratory heat and water exchange: physiological and clinical implications. J Appl Physiol Respir Env Exerc Physiol. 1983;54(2):331–6.

[20] Fang L, Clausen G, Fanger PO. Impact of temperature and humidity on perception. Indoor Air. 1998;8:80–90. doi: 10.1111/j.1600-0668.1998.t01-2-00003.

[21] IPCC Türkiye Raporu. National Inventory Report (NIS) - TURKEY Greenhouse Gas Inventory, 1990 to 2005. Ankara, Türkiye: 2007.

[22] Haksevenler T. İstanbul'da farklı iç ortamlarda hava kalitesinin belirlenmesi. İstanbul Üniversitesi Fen Bilimleri Enstitüsü, Yüksek Lisans Tezi. İstanbul, Türkiye; 2010.
[23] Wilson WE, Chow JC, Claiborn C, Fusheng W, Engelbrecht J, Warson JG. Monitoring of particulate matter outdoors. Chemosphere. 2002;49:1009–43.
[24] Onat B, Stakeeva B. Assessment of fine particulate matters in the subway system of Istanbul. Indoor Built Env. 2014;23:574–83.
[25] Onat B, Stakeeva B. Personal exposure of commuters in public transport to PM2. 5 and fine particle counts. Atmos Pollut Res. 2013;4(3):329–35.63.
[26] Onat B, Şahin ÜA, Sivri N. The relationship between particle and culturable airborne bacteria concentrations in public transportation. Indoor Built Environ. 2017;26(10):1420–8.
[27] Onat B, Şahin ÜA, Uzun B, Akın Ö, Özkaya F, Ayvaz C. Determinants of exposure to ultrafine particulate matter, black carbon, and PM2.5 in common travel modes in Istanbul. Atmos Environ. 2019;206:258–70.
[28] Lohmann U, Feichter J. Global indirect aerosol effects: A review. Atmos Chem Phys. 2005;5(3):715–37.
[29] Kahraman O, Dündar C. Toz taşınımı olayının uzaktan algılama ve sayısal tahmin modeli ile analizi. Ege Coğrafya Dergisi. 2014;23(2):53–64. İzmir, Türkiye.
[30] USEPA (2008). Characteristics of particles–Particle Size Categories. EPA.gov (Erişim Tarihi: 14.12.2023).
[31] Passi A, Nagendra SMS, Maiya MP. Characteristics of indoor air quality in underground metro stations: A critical review. Build Environ. 2021;198:107907. doi: 10.1016/j.buildenv.2021.107907.